

INFLUENCE OF NEAR-SURFACE MOUNTED FRP WITH CEMENTITIOUS MATERIAL ON OUT-OF-PLANE BEHAVIOR OF REINFORCED MASONRY WALLS

ZUHAIR ALJABERI and JOHN J. MYERS

*Dept of Civil, Architectural & Environmental Engineering,
Missouri University of Science and Technology, Rolla, USA*

Eight medium scale reinforced masonry walls were built as a part of this study. These reinforced walls were strengthened using carbon fiber reinforced polymer [FRP] (bars and tapes) and glass FRP (bars) using a near surface mounted technique (NSM) with cementitious material; constant mild steel reinforcement ratio (ρ) was used. These strengthened walls were supported as a simply supported wall under an out-of-plane cyclic load applied along two line loads. This study presented the effect of different parameters, these parameters related to FRP (type and amount), bond pattern (stack and running), and existing of FRP in compression face of the walls. This paper reveals the relation between these factors and the out-of-plane capacity of the reinforced wall strengthened with FRP. Different modes of failure occurred in the strengthened reinforced walls, including a punching shear failure through the concrete block, crushing of concrete block and debonding of FRP reinforcement from the masonry substrate.

Keywords: Strengthening, Overloading, Fiber reinforced polymer, NSM, Carbon fiber.

1 INTRODUCTION

Masonry walls are commonly used throughout the world because they are inexpensive and easily constructed. Many unreinforced masonry (URM) structures are damaged when subjected to overloading, earthquake and wind loads. An effective technique was needed to strengthen reinforced masonry structures against overloading conditions in order to improve both the load carrying capacity and ductility within a masonry wall. An attractive method for strengthening application is using FRP composites as a near surface mounted (NSM) system. An FRP reinforcement is lightweight and available in multiple forms, many of which could easily be manipulated to match variable structural shapes and geometries (ACI 440.2R-10). The use of epoxy has proven to give excellent performances both in terms of bonding and durability. FRP with epoxy has some drawbacks, poor behavior of the resin at temperatures above the glass transition temperature, emission of toxic fumes, moisture impermeability (Hashemi *et al.* 2008). Using a cementitious material as an alternative adhesive agent is very attractive and eliminates these drawbacks. This investigation evaluates the behavior of reinforced masonry wall strengthened with FRP composites using cementitious based material.

2 TESTING PROGRAM

This study was undertaken using FRP NSM composites as a strengthening system. The system consisted of the installation of FRP reinforcing bars in slots that had been grooved into the masonry tension surface, as presented in Figure 1. Both E-glass and carbon fiber were used.



Figure 1. Installation of FRP bars in grooves.

2.1 Test Matrix

This study was conducted to investigate the effectiveness of strengthening of reinforced masonry walls using FRP with cementitious material considering several variables as shown in Table 1. Eight reinforced masonry walls were constructed for this experimental program using full grouted concrete blocks with a Type S mortar. The nominal dimensions of these walls were 48 in. length by 24 in. width and the nominal thickness 6 in. Each specimen was reinforced with 2 #4 mild reinforcing bars. The specimens were constructed in running and stack bond. The walls were grouted four days after construction to ensure stability during the vibration process. They were strengthened with Aslan 500 CFRP tape size 2 (0.08 x 0.63) in. [(2 x 16) mm], Aslan 200 CFRP bar size 2 (1/4) in. [(6.35) mm], and Aslan 100 GFRP Rebar size 2 (1/4) in. [(6.35) mm]. The test was done after at least 28 days as a curing period.

2.2 Specimen Designation

The specimen ID includes two parts: the first part consists of three characters that represent the FRP information (type, shape, and size). The first character identified the FRP type: namely “C” for carbon FRP and “G” for glass FRP. The second character referenced the bars cross section; an “S” represents a rectangular tape, and a “B” represents a circular bar. The third character represents the FRP size. The second part of the ID identifies the wall bond pattern and the number of FRP bars. The first character represented the wall bond pattern applied: “R” for running and “S” for stack. The second character referred to the number of bars.

2.3 Material Properties

A series of tests were performed to determine each material’s mechanical properties. The properties of the materials that were used to construct the specimens are

summarized in Table 2. The manufacture properties of CFRP and GFRP bar are presented in Table 3.

Table 1. Experimental test matrix.

Wall	Specimen ID	Type of FRP	Bar Size	Number of Bars	Bond Pattern	FRP Bar Dimension, in.(mm)	Groove Dimension, in.(mm)
1	Control				running		
2	Control				Stack		
3	CS2-R1	Carbon tape	2	1	running	0.08x0.63 (2x16)	0.5*1.25 (12.7x31.75)
4	CB2-R1	Carbon bar	2	1	running	1/4 (6.35)	0.6 (15.25)
5	GB2-R1	Glass bar	2	1	running	1/4 (6.35)	0.6 (15.25)
6	GB2-R2	Glass bar	2	2	running	1/4 (6.35)	0.6 (15.25)
7	GB2-S2	Glass bar	2	2	Stack	1/4 (6.35)	0.6 (15.25)
8	GB2-R2*	Glass bar	2	2	running	1/4 (6.35)	0.6 (15.25)

* This specimen has one bar in tension and other in compression

Table 2. Results of the material properties.

Item	Properties	Values	Method
Concrete block	Prism compressive strength (psi)	3000	ASTM C1314-12
Mortar type S	Compressive strength (psi)	2500	ASTM C109-13
Grout	Compressive strength (psi)	4985	ASTM C1019-13
Cementitious material	Compressive strength (psi)	7760	ASTM C1019-14
Steel bar	Yield strength (psi)	67250	ASTM A370-13
	Modulus of Elasticity	29 E+06	

Table 3. Mechanical properties of FRP.

Type of FRP	Dimension (in) (mm)	Average Maximum Stress ksi.(MPa)	Average Maximum Strain %	Average Tensile Modulus of Elasticity (MOE) ksi. (GPa)
Aslan 500 CFRP tape	0.08x0.63 (2x16)	325 (2275)	1.81	18000 (124)
Aslan 200 CFRP bar	1/4 (6.35)	325 (2275)	1.81	18000 (124)
Aslan 100 GFRP bar	1/4 (6.35)	130 (910)	1.94	6700 (46)

2.4 Test Setup

Four-point line loading with simply supported boundaries can be used to conduct out-of-plane testing of reinforced masonry walls as shown in Figure 2. An MTS double-acting hydraulic jack with a push-pull capacity of 140 kips (965 MPa) was used for applying load. This load was transferred to the masonry specimen by means of continuous steel plates and bars along the full width of the external face of reinforced walls to provide two equal line loads. The distance between these two lines was 8 in. (200 mm). The load was applied in half-cycles of loading and unloading, as a displacement control at a rate of 0.05 in. /min (1.25 mm/min).The displacement amplitude increment was 0.25 in. (6.35 mm) and a double half loading cycle was applied for each amplitude level as illustrated in Figure 3. Deflections at mid and third span were measured using three (LVDTs) at each side in addition to placed strain gauges on the FRP bars and steel bar to record their strains during the loading.



Figure 2. Test setup.

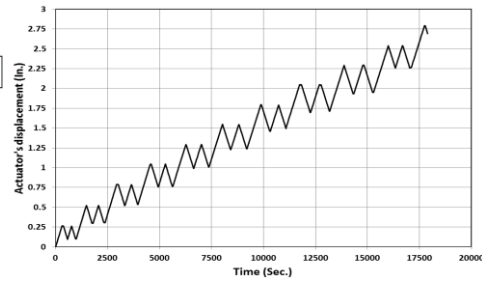


Figure 3. Displacement history.

3 RESULTS AND DISCUSSION

3.1 Modes of Failure

This investigation present different modes of failure occurred during the test. Debonding of FRP reinforcement from the masonry substrate is a general failure mode. This failure mode followed by punching shear through the concrete block, crushing of concrete and flexure–shear as shown in Figure 4.



Figure 4. Observed modes of failure.

3.2 General Behavior of Strengthened Masonry Wall

Reinforced concrete masonry walls generally behave in a flexural ductile mode as a result of their steel reinforcement. The load–deflection relationship was approximately bi linearly prior to the load of yield point. The first flexural tensile crack was initiated at the block mortar in the maximum moment region. Further flexural tensile cracks developed during loading, beyond the cracking load. The CFRP reinforcement and large amount of GFRP reinforcement (in this study 2 bar) that was encapsulated with cementitious material caused cracks to propagate in masonry units. Since the tensile stresses at the mortar joints were being taken by FRP reinforcement, a redistribution of stress occurred (Galati *et al.* 2006). The masonry cracks were oriented at 45°. For the other specimen the cracks extended along the bed joints and grooves as the load increased. As a result of cementitious cracking, the embedding material deteriorated gradually and the failure in general is debonding. Flexural shear and shear cracks outside the constant moment region in addition to concrete unit crushing were generated in later stages of loading.

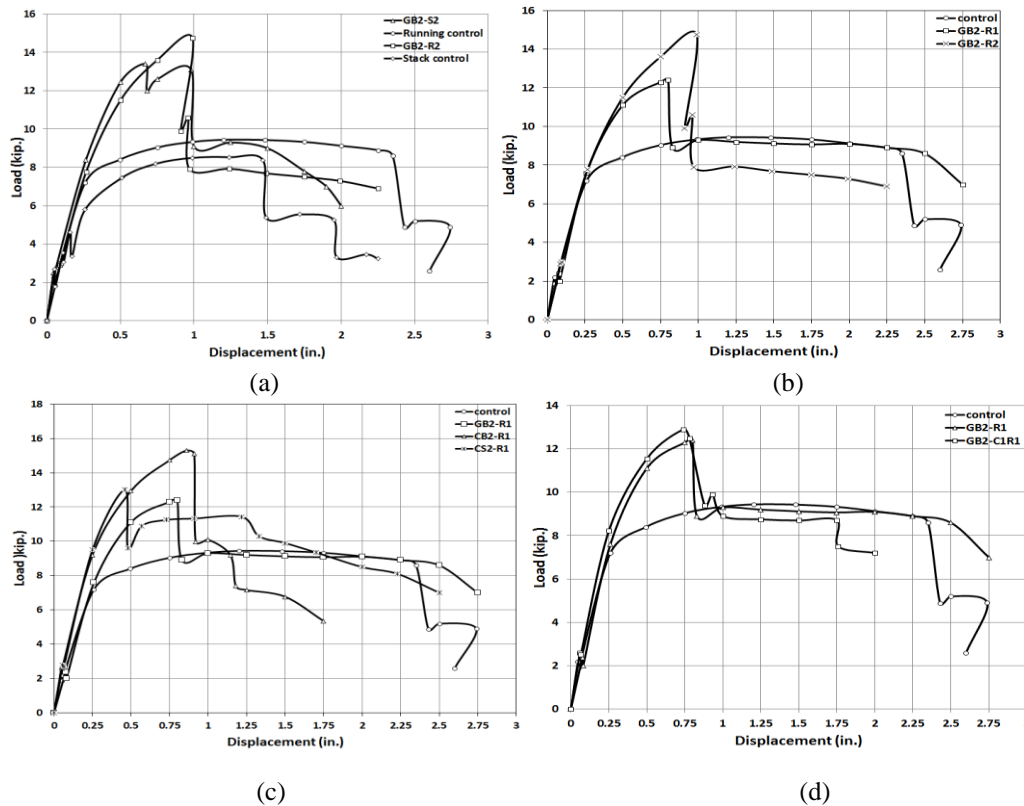


Figure 5. Load versus deflection curves for test specimens.

3.3 Discussion of Results

The envelope load vs. deflection curves for specimens are illustrated in Figure 5. For all specimens, the moment capacity and stiffness of the reinforced walls strengthened with FRP increased (as compared to the control specimen). Interestingly, the wall's capacity dropped to approximately the same capacity of the control specimen after the post - peak behavior occurred. Then the walls capacity dropped below the control specimen capacity; this is due to existing of block unit cracking and damage accumulation after failure occurred. An interesting point for the specimen strengthened with carbon tape is the sliding inside the groove was happened. This sliding develops a flexure capacity after debonding more than the capacity of control specimen due to friction force developed. The load-deflection responses for specimens CB2-R1, CB2-R1, CS2-R1 and the control specimen are illustrated in Figure 5(a). A significant difference occurred in the slope of the second portion of the response. The GB2-R1 specimen was less stiff than the others, thus illustrating the effect of the specimen strengthened with GFRP compared to CFRP. The FRP composite that was added as an NSM significantly increased not only the out-of-plane load carrying capacity but also its stiffness. From Figure 5(b) the percent of the capacity increase can be determined and its ranges from 131%–162% times the flexural capacity of the control reinforced

wall. The moment capacity in both the GB2-R1 and the GB2-R2 increased as the FRP increased. Also, debonding is the mode of failure for both of them. The bond pattern effect is illustrated in Figure 5(c). The stack and running pattern's behave as the same response in terms of ductility but the running specimen got a little more flexural capacity. The behavior of stack specimen improved when the head joint was reinforced with an FRP bar. Specimens GB2-R2 and GB2-R2* shown in Figure 5(d) exhibited a similar response. The existing of compression reinforcement had a very little effect on stiffness and flexural capacity. That's happened due to high FRP reinforcement ratio and the strain in compression FRP not exceed 5% of the maximum strain in tension side. This factor requires further study with specimens that have different FRP reinforcement ratios.

5 CONCLUSION

The strengthened reinforced masonry wall's behavior was significantly dependent on the type of FRP used. A wall strengthened with GFRP bar and CFRP tape had more displacement ductility than did the same wall strengthened with CFRP bar due to high stiffness of CFRP and sliding possibility of tape. The flexural capacity was increased between 131% and 162% when NSM was used compared to the control wall. The failure mode was identified from the test results as a debonding failure. The behavior of stack specimen was improved significantly by adding a joint FRP reinforcement. Finally, the existing of compression reinforcement yielded minimal effect on stiffness and flexural capacity.

Acknowledgement

The authors wish to acknowledge the support of Midwest Block & Brick in Jefferson City, Missouri and Hughes Brothers in Seward, Nebraska. The authors also wish to thank the technical support from the CArEE Department and CIES at Missouri S & T.

References

- ACI 440.7R-10, Guide for the Design and Construction of Externally Bonded Fiber Reinforced Polymer Systems for Strengthening Unreinforced Masonry Structures, *ACI*, 2010, 30 pp.
- Galati, N., Tumialan, G., and Nanni, A., Strengthening with FRP bars of URM walls subject to out-of-plane loads, *Construction and Building Materials*, June, 2005 pp.105.
- Hashemi, S. and Al-Mahidi, R., Cement Based Bonding Material for FRP, *11th Int. Inorganic-Bonded Fiber Composites Conference (IIBCC)*, Madrid, Spain, Nov. 5-7, 2008 pp.267.